

Supplementary materials

Striatal dopamine mediates the interface between motivational and cognitive control in humans: Evidence from genetic imaging

Esther Aarts, Ardi Roelofs, Barbara Franke, Mark Rijpkema, Guillén Fernández, Rick C. Helmich, Roshan Cools

Correspondence should be addressed to Esther Aarts, Donders Institute for Brain, Cognition and Behaviour, Radboud University Nijmegen, The Netherlands. Email address: e.aarts@donders.ru.nl

SUPPLEMENTARY METHODS

Participants

Initially, 24 participants were scanned. One participant was excluded due to technical problems during scanning, one participant's saliva sample was not collected, genotyping of one participant's saliva sample failed, and one participant had a *DAT1* allele different from the two alleles we were interested in. The remaining sample size was 20.

Task

The targets of the Stroop-like task-switch paradigm consisted of written words in arrows. The lines and letters of the targets were white on a black background (**Figure 1, main text**). Participants responded manually to the Stroop-like stimuli by pressing a left button (with their left middle finger) or a right button (with their left index finger) on a scanner-compatible button box. This button-box response was done with the left hand (right motor cortex) because the stimuli themselves were language-related (left hemisphere).

The intervals between the reward-cue and the task-cue, the task-cue and the target, and between the feedback and the reward-cue of the next trial were jittered with a variable delay between 2 and 6 seconds. Feedback was given immediately after the participant's response. The cues and the feedback remained on the screen for 600 ms. Targets remained on the screen until a response was made or until the end of the individually determined response window.

The response deadline was calculated for each participant separately, on the basis of their performance in two practice blocks in the scanner during the anatomical scan. Both practice blocks consisted of 12 word-task trials and 12 arrow-task trials, half of which were repeat trials and half of which were switch trials. In the practice block, no reward-cues appeared and no

feedback was given. Each practice block lasted for about 4 minutes. Before the second practice block, participants were instructed to respond as quickly (yet accurately) as possible. The mean response times (RT) of the correct trials per trial-type (arrow-repeat, arrow-switch, word-repeat, word-switch) from the second practice block were taken as a response deadline in the main experiment. When participants responded faster for a certain trial-type in the first practice block, this mean RT was taken instead of the one from the second practice block.

In the main experiment, a white asterisk was displayed during the variable intervals between the reward-cue and the task-cue and between the task-cue and the target. In the inter-trial interval, a blue asterisk was displayed. Participants were told to fixate on the asterisks.

The maximum amount of money a participant was able to win was 8.80 Euros. On average, the participants won 7 Euros. At the end of the experiment, the total amount of awarded money was shown on the screen and this was transferred to the participant's bank account together with the standard compensation that was earned for participating in the fMRI experiment (15 euros).

Genotyping

All molecular genetic analyses were carried out in a CCKL-certified laboratory at the department of Human Genetics of the Radboud University Nijmegen Medical Centre. DNA was isolated from saliva samples using Oragene kits (DNA Genotek Inc, Ottawa, Ontario, Canada). Genotyping of the 40 base pair variable number of tandem repeats (VNTR) polymorphism in the 3' untranslated region (UTR) of the *SLC6A3/DAT1* gene encoding the DAT has been described before (Kooij *et al*, 2008). For *DAT1*, two genotype groups were established: 11 participants (55% female, mean age: 21.6) were homozygous for the common 10-repeat allele (10R

homozygotes) and 9 participants (44% female, mean age: 22.4) were heterozygous for the 9-repeat allele (9R carriers).

We also genotyped the catechol-*O*-methyltransferase gene *COMT* rs4680 (Val^{108/158}Met) single nucleotide polymorphism. Genotyping was performed using Taqman analysis (assay ID: Taqman assay: C__25746809_50; reporter 1: VIC-A-allele; Applied Biosystems, Nieuwerkerk a/d IJssel, The Netherlands). Genotyping was carried out in a volume of 10 µl containing 10 ng of genomic DNA, 5 µl of ABgene Mastermix (2x; ABgene Ltd., Hamburg, Germany), 0.125 µl of the Taqman assay and 3.875 µl of H₂O. Amplification was performed on a 7500 Fast Real-Time PCR System starting with 15 minutes at 95°C, followed by 50 cycles of 15 seconds at 95°C, 1 minute at 60°C. Genotypes were scored using the algorithm and software supplied by the manufacturer (Applied Biosystems). For *COMT*, participants were classified as having two (Met/Met; n = 2), one (Val/Met; n = 13), or no Met-alleles (Val/Val; n = 5). The *DATI* 10R/10R group consisted of 2 Met/Met participants, 7 Val/Met participants, and 2 Val/Val participants. The *DATI* 9R/10R group consisted of 6 Val/Met participants and 3 Val/Val participants.

To investigate the random genotyping error rate in the analyses of *DATI* and *COMT*, the lab included 5% duplicate DNA samples, which had to be 100% consistent. In addition, 4% blanks were included, which were required to be negative.

fMRI preprocessing

Data were pre-processed and analyzed using SPM5 (Wellcome Dept. of Cognitive Neurology, London). The first four volumes of each participant's data set were discarded to allow for T1 equilibrium. First, functional EPI images were spatially realigned using a least squares approach and a 6 parameter (rigid body) spatial transformation. Subsequently, the time-

series for each voxel was realigned temporally to acquisition of the middle slice. Images were normalized to a standard EPI template centered in MNI space (Ashburner and Friston, 1997) by using 12 linear parameters and resampled at an isotropic voxel size of 2 mm. The normalized images were smoothed with an isotropic 8 mm full-width-at-half-maximum (FWHM) Gaussian kernel. Anatomical images were spatially coregistered to the mean of the functional images (Ashburner *et al*, 1997) and spatially normalized by using the same transformation matrix applied to the functional images.

Structural MRI analysis

First, an automatic subcortical segmentation method was applied to the structural MRI scans using FSL 4.1 First v1.1 software (FMRIB, Oxford, UK). After automatic segmentation, volume information of the subcortical structures of interest (left and right nucleus accumbens, left and right caudate nucleus, and left and right putamen) was extracted from the segmentation results using a script written in Matlab7.2. To correct the volume of the subcortical structures for total brain volume, we performed a standard segmentation of the anatomical data into grey matter, white matter, and cerebrospinal fluid using SPM. Total brain volume was defined as the grey matter plus white matter volume and used to express the subcortical volumes as percentages. Independent t-tests were performed on these striatal volumes to test for differences between the groups.

SUPPLEMENTARY RESULTS

Behavioral Results

During scanning, we measured error rates and response times (RTs) as a function of reward magnitude (i.e., 10 cents or 1 cent) as well as trial-type (task repeat or task switch) in a Stroop-like task-switch paradigm (**Figure 1, main text**). **Table S1** displays the mean RTs for the correct trials and error rates.

Analyses of error rates revealed only a marginal main effect of reward [$F(1,18) = 3.4, P = .08, \eta_p^2 = .17$], but a significant reward x *DATI* interaction (see main text). In general, participants made more errors on switch trials than on repeat trials [$F(1,18) = 16.2, P = .001, \eta_p^2 = .47$], and while this switch cost did not interact with reward [$F < 1$], there was a significant interaction between *DATI*, reward and trial-type (see main text). There was no overall main effect of *DATI* on the error rates [$F(1,17) < 1$].

In terms of reaction times (RTs, see **Table S1**), participants responded significantly faster on high reward than on low reward trials, thus revealing a reward benefit [$F(1,18) = 8.4, P = .01, \eta_p^2 = .32$]. They also responded significantly faster on repeat than on switch trials, thus revealing a switch cost [$F(1,18) = 12.4, P = .002, \eta_p^2 = .41$]. Reward and trial-type did not interact [$F(1,17) = 1.2, P = .29, \eta_p^2 = .07$]. Further there were no reward x *DATI*, trial-type x *DATI*, or reward x trial-type x *DATI* interactions [all $F(1,17) < 1.5$]. In contrast to the error rates, there was a marginal main effect of *DATI* on RTs [$F(1,17) = 3.8, P = .068, \eta_p^2 = .18$] meaning that 9R carriers responded overall faster than 10R homozygotes.

Functional imaging results

Whole-brain analyses

Main effects of reward during anticipation (reward- and task-cues) and receipt are shown in **Tables S2 and S3** (and **Figure 3a**, main text). As predicted, main reward effects were

observed in the bilateral ventral striatum (at our statistical threshold of $P < 0.05$ cluster level, corrected for multiple comparisons over the whole brain), during both reward-cues (centered on the ventromedial striatum [nucleus accumbens]), and task-cues (centered on the ventrolateral striatum [putamen]). During reward receipt, the bilateral ventral striatum (centered most laterally on the ventrolateral striatum [putamen]) was more active during positive feedback (the word “good” + the earned reward in cents for correct and quick responses) than during negative feedback (the words “error” + “0 cents” for erroneous trials), although there were no differences between high- and low-reward at receipt. Thus, dependent on the task phase, we observed a medial-to-lateral gradient in the ventral striatum (**Figure 3a**, main text), with reward anticipation during reward-cues eliciting ventromedial striatal activity (i.e., nucleus accumbens), reward anticipation during the subsequent task-cues eliciting more lateral activity in the ventral striatum, and reward receipt during feedback eliciting most lateral activity in the ventral striatum (i.e., ventral putamen). Conversely, negative feedback induced more activity in a frontal and temporal-parietal network than did positive feedback, while no striatal activity was observed for this contrast (**Table S3**).

There were no significant main trial-type or trial-type x reward effects during task-cues or targets irrespective of *DATI* in the striatum or PFC. During task-cues we only observed a main trial-type effect in a cluster (of 170 voxels) in the middle occipital gyrus, including part of the inferior parietal lobe (peak: $x = -28, y = -66, z = 40, T = 5$). There were no trial-type x *DATI* effects during task-cues or targets in the striatum or PFC, irrespective of reward, although a trial-type x *DATI* effect in subgenual ACC (peak: $x = 8, y = 22, z = -6, T = 8.1$; 125 voxels) reached significance at the whole-brain level.

Anatomical ROI analyses

Caudate nucleus

During the task-cues, we observed a main effect of reward [left: $F(1,18) = 14.17, P = .001, \eta_p^2 = .44$; right: $F(1,18) = 30.16, P < .001, \eta_p^2 = .63$], but no reward x *DATI* [left: $F(1,18) < 1$; right: $F(1,18) = 2.14, P > .05, \eta_p^2 = .11$] or reward x trial-type x *DATI* [left and right: $F(1,18) < 1$] interactions. Thus, the reported three-way interaction effect in the striatum was present only during targets and not during task-cues.

During the targets, there was no reward x trial-type interaction irrespective of *DATI* [reward x trial-type: $F(1,18) < 1$] and no other interaction or main effects.

Table S1 shows the mean beta-weights of the left anatomical caudate nucleus ROI during targets. To assess the three-way interaction effect further (see main text), we analyzed whether the *DATI*-dependent effect of anticipated reward on switch-related activity in the caudate nucleus was attributable to modulation of activity during switch trials or repeat trials. The simple reward x *DATI* interaction effect was non-significant on either repeat trials [$F(1,18) = 2.61, P = .12, \eta_p^2 = .13$] or switch trials [$F(1,18) = .08$]. Thus, 9R carriers benefited to a greater extent than the 10R homozygotes from high relative to low reward only in terms of the difference between switch and repeat trials. It might be noted that effects of reward on BOLD differences are easier to interpret than effects of reward on absolute BOLD signal, given possible non-specific effects of reward on BOLD signal.

Finally, there were no significant main effects of reward receipt [left: $F(1,18) = 2.19, P > .05, \eta_p^2 = .11$; right: $F(1,18) < 1$] or reward x *DATI* interactions during receipt [left: $F(1,18) = 2.89, P > .05, \eta_p^2 = .14$; right: $F(1,18) < 1$].

Putamen

By contrast to analysis of the caudate nucleus data, analysis of the putamen data revealed a significant main effect of reward (valence) [left: $F(1,18) = 9.56, P = .006, \eta_p^2 = .35$; right: $F(1,18) = 6.40, P = .021, \eta_p^2 = .26$] and a significant reward x *DATI* interaction [left: $F(1,18) = 5.46, P = .031, \eta_p^2 = .23$; right: $F(1,18) = 4.93, P = .039, \eta_p^2 = .21$] during receipt, but not during reward cues [main reward effects: left: $F(1,18) = 1.82, P > .05, \eta_p^2 = .09$; right: $F(1,18) = 1.67, P > .05, \eta_p^2 = .08$; reward x *DATI* effects: left: $F(1,18) = 3.78, P > .05, \eta_p^2 = .17$; right: $F(1,18) = 1.08, P > .05, \eta_p^2 = .06$] or task-cues [left: $F(1,18) = 3.14, P > .05, \eta_p^2 = .15$; right: $F(1,18) < 1$; reward x *DATI* effects: left: $F(1,18) = 1.12, P > .05, \eta_p^2 = .06$; right: $F(1,18) < 1$]. There was no reward x trial-type x *DATI* interaction during the targets [left: $F(1,18) = 1.73, P > .05, \eta_p^2 = .09$; right: $F(1,18) < 1$] and no *DATI* effects as a function of reward magnitude (high vs low) rather than valence (positive vs. negative).

SUPPLEMENTARY DISCUSSION

The opposite effects of *DATI* genotype on striatal activity during anticipation and receipt are reminiscent of previously observed dopaminergic modulation of striatal activity associated with the reward prediction error during learning (Pessiglione *et al*, 2006). Given that they exhibit enhanced striatal activity during reward anticipation, it is possible that the reduced receipt-related activity in the 9R carriers reflects reduced surprise upon reward receipt. However, it should be noted that in this experiment, which did not involve any learning, anticipatory activity and receipt-related activity were localized in different medial and lateral regions of the striatum, thus indicating that they are unlikely to reflect modulation of a process mediated by a single mechanism. Moreover the functional opponency between the reward effects is not perfect, given

that it reflects a modulation of reward magnitude during anticipation, but of reward valence during reward receipt. Instead, the contrasting effects of *DATI* genotype on striatal BOLD activity during anticipation versus receipt of reward demonstrate opposite effects of dopamine on preparatory and consummatory reward processes (see Discussion main text). Furthermore, these opposite genotype effects during anticipation and receipt imply that there is not always a one-to-one mapping between dopamine processing and BOLD (as observed in Knutson and Gibbs, 2007).

In contrast to reward anticipation, reward receipt impaired task switching (**Figure S1**). It should be noted that this effect might reflect reduced cognitive flexibility after positive feedback, or alternatively, enhanced cognitive flexibility after negative feedback, consistent with prior observations of error-induced recruitment of cognitive control (Ridderinkhof *et al*, 2004). While the current experiment was not designed to directly test this hypothesis (see Figure S1), future studies may assess whether these feedback-induced effects on task switching are modulated by striatal dopamine.

SUPPLEMENTARY REFERENCES

Ashburner J, Friston K (1997). Multimodal image coregistration and partitioning--a unified framework. *Neuroimage* **6**(3): 209-217.

Knutson B, Gibbs SE (2007). Linking nucleus accumbens dopamine and blood oxygenation. *Psychopharmacology (Berl)* **191**(3): 813-822.

Kooij JS, Boonstra AM, Vermeulen SH, Heister AG, Burger H, Buitelaar JK, *et al* (2008). Response to methylphenidate in adults with ADHD is associated with a polymorphism in SLC6A3 (DAT1). *Am J Med Genet B Neuropsychiatr Genet* **147B**(2): 201-208.

Pessiglione M, Seymour B, Flandin G, Dolan RJ, Frith CD (2006). Dopamine-dependent prediction errors underpin reward-seeking behaviour in humans. *Nature* **442**(7106): 1042-1045.

Ridderinkhof KR, Ullsperger M, Crone EA, Nieuwenhuis S (2004). The role of the medial frontal cortex in cognitive control. *Science* **306**(5695): 443-447.

Table S1. Mean response times (RT) in ms, error rates (ERR) in percentages, and beta-weights (betas) of the left anatomical caudate ROI. Standard errors of the mean in brackets.

<i>DATI</i>	REWARD	TRIAL-TYPE	RT	ERR	betas
10R/10R	high	repeat	450 (4.67)	7.1 (1.2)	3.48 (0.77)
		switch	467 (5.4)	14.5 (1.6)	3.40 (0.72)
	low	repeat	460 (5.4)	7.7 (1.3)	3.30 (0.76)
		switch	476 (6.0)	12.2 (1.5)	3.52 (0.78)
9R/10R	high	repeat	414 (4.9)	6.6 (1.3)	3.45 (0.85)
		switch	431 (6.1)	10.7 (1.6)	3.58 (0.90)
	low	repeat	419 (6.2)	8.8 (1.5)	3.92 (1.03)
		switch	457 (8.0)	17.7 (2.0)	3.57 (1.05)

Table S2. MNI stereotactic coordinates of local maxima for clusters with greater activity for high- than for low-reward trials during reward cues, during task-cues and the interaction between reward and *DAT1* genotype.

Region	cluster statistics			local maximum			
	size	p-value	T-value	x	y	z	
<i>Reward cues: high > low</i>							
inferior occipital gyrus	L	9216	<0.001	9.55	-30	-92	0
Superior occipital gyrus	R			9.3	24	-76	32
middle occipital gyrus	L			8.88	-16	-100	6
nucleus accumbens	R	1548	<0.001	6.54	10	8	-2
nucleus accumbens	L			5.82	-12	8	-8
Thalamus	R			5.8	4	-4	6
pre-supplementary motor area	L	400	<0.001	5.47	-8	14	56
medial superior frontal gyrus	L			5.38	-6	14	48
pre-supplementary motor area	R			4.97	6	0	62
middle frontal gyrus	L	187	0.001	5.25	-32	52	16
superior frontal gyrus	R	129	0.012	6.57	32	56	20
<i>Task cues: high > low</i>							
superior frontal gyrus	R	3486	<0.001	9.33	26	-2	68
pre-supplementary motor area	R			8.39	6	8	52

ventral putamen	L	1667	<0.001	9.54	-18	14	-4
Midbrain	L			7.29	-8	-20	-16
Hippocampus	L			5.98	-14	-8	-10
ventral putamen	R	754	<0.001	8.09	20	14	-8
nucleus accumbens	R			6.63	14	8	-8
caudate nucleus	R			5.71	6	6	14
inferior parietal lobe	L	531	<0.001	6.27	-38	-56	60
Precuneus	R	440	<0.001	6.41	14	-68	56
Insula	R	340	<0.001	5.54	42	16	-2
inferior frontal gyrus (p. orbitalis)	R			5.25	44	26	0
Precuneus	L	313	<0.001	6.5	-8	-72	48
Cerebellum	R	167	0.005	6.27	2	-54	-12

Reward cues: (high > low) x (DAT 9/10 > 10/10)

Cerebellum	L	2316	<0.001	7.54	-10	-48	-2
fusiform gyrus	L			6.65	-22	-44	-12
Cerebellum	R			6.64	14	-56	-6
superior occipital gyrus	R	1396	<0.001	7.86	26	-74	30
middle occipital gyrus	R			7.16	30	-84	28

middle occipital gyrus	L	646	<0.001	6.69	-32	-78	24
superior parietal lobe	L			4.95	-22	-70	46
middle frontal gyrus	L	373	<0.001	5.97	-32	0	60
precentral gyrus	L			5.85	-34	-10	58
Thalamus	L	324	<0.001	5.42	-8	-4	6
Midbrain	L			5.11	-12	-26	-4
Precuneus	R	115	0.021	5.56	12	-46	48
middle frontal gyrus	L	99	0.041	4.67	-32	56	16

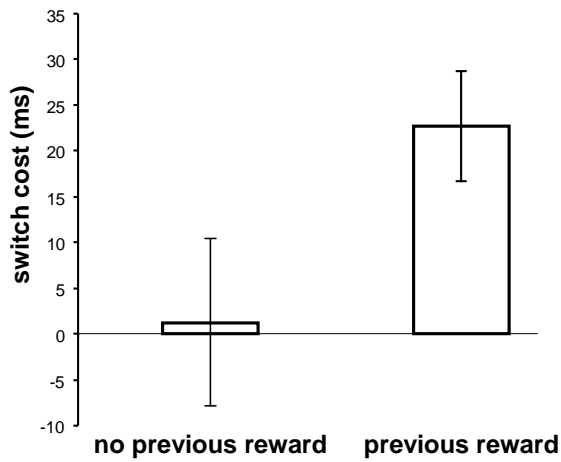
Table S3. MNI stereotactic coordinates of local maxima for clusters with greater activity for feedback related to correct responses than for feedback related to incorrect responses, and vice versa.

Region	cluster statistics			local maximum			
	size	p-value	T-value	x	y	z	
<i>Feedback: correct > incorrect</i>							
caudate nucleus	R	378	<0.001	6.97	18	12	20
caudate nucleus	L	232	0.001	6.08	-18	0	28
Putamen	L			4.41	-26	-10	14
ventral putamen	L	138	0.015	5.83	-18	2	-14
<i>Feedback: incorrect > correct</i>							
inferior frontal gyrus (p. orbitalis)	R	7259	<0.001	8.16	40	22	-16
inferior frontal gyrus (p. triangularis)	R			7.62	54	28	22
superior temporal gyrus	R			7.54	62	-50	20
inferior frontal gyrus (p. orbitalis)	L	5376	<0.001	11.32	-28	18	-16
inferior frontal gyrus (p. triangularis)	L			9.94	-44	16	20
anterior cingulate cortex	L	5375	<0.001	8.31	-8	26	30
anterior cingulate cortex	R			8.3	6	34	28
medial superior frontal gyrus	L			7.87	-6	20	48
inferior parietal lobe	L	3424	<0.001	7.29	-30	-54	48
middle temporal gyrus	L			6.96	-66	-48	2

Thalamus	L	3012	<0.001	7.39	-10	-12	8
Thalamus	R			7.05	8	-14	10
				6.57	-10	-14	-12
calcarine gyrus	R	1145	<0.001	4.74	4	-82	12
calcarine gyrus	L			4.7	-2	-90	10
lingual gyrus	L			4.59	-12	-78	6
Precuneus	L	645	<0.001	6.69	-4	-62	46
Precuneus	R			6.22	8	-56	46
superior frontal gyrus	R	200	0.002	6.16	18	52	30
middle orbitofrontal gyrus	R			4.54	32	50	4

FIGURE S1

A) Switch cost in response times



B) Switch cost in error rates

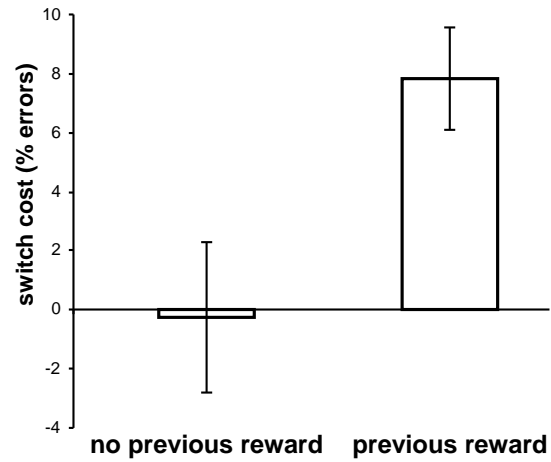


Figure S1. Behavioral switch cost as a function of previous reward.

The switch cost (switch – repeat) increased in terms of both response times (a) and error rates (b) when participants had earned reward (1 or 10 cents) on the previous trial compared to when participants had made an error or did not respond in time on the previous trial (0 cents). Error bars represent standard errors of the difference between switch and repeat trials.

Note that the data in the figure represents all subjects, whereas the complete GLM (with all factors) contains missing cells because the previous reward factor is dependent on the behavior of participants (i.e., correct or incorrect responding). Therefore, the statistics in the main text is done on fewer participants (response times: 7 DAT 10/10 participants, 5 DAT 9/10 participants; error rates: 9 DAT 10/10 participants, 7 DAT 9/10 participants).

For that same reason we did not have sufficient power to assess effects of *DAT1* genotype as a function of previous reward and/or to assess neural effects of previous reward.